Passivation of acceptors in GaN by hydrogen and their activation

Michael A. Reshchikov*, Oleksandr Andrieiev, Mykhailo Vorobiov, Dexian Ye, and Denis O. Demchenko

Department of Physics, Virginia Commonwealth University, Richmond, VA 23220, USA

Benjamin McEwen and Shadi Shahedipour-Sandvik

College of Nanoscale Science and Engineering, SUNY-Albany, Albany, New York 12203, USA

Abstract

GaN is an important semiconductor for energy-efficient light-emitting devices. Hydrogen plays a crucial role in gallium nitride (GaN) growth and processing. It can form electrically neutral complexes with acceptors during growth, which significantly increases the acceptor incorporation. Post-growth annealing dissociates these complexes and is widely utilized for activating Mg acceptors and achieving conductive *p*-type GaN. In this work, we demonstrate that other acceptors, such as C and Be, also form complexes with hydrogen similar to Mg. The effect of thermal annealing of GaN on photoluminescence (PL) was investigated. In samples moderately doped with Be, the Be_{Ga}-related yellow luminescence (YL_{Be}) band intensity decreased by up to an order of magnitude after annealing in N_2 ambient at temperatures T_{ann} = 400–900 °C. This was explained by the release of hydrogen from unknown traps and the passivation of the Be_{Ga} acceptors. A similar drop of PL intensity at T_{ann} = 350–900 °C was observed for the C_N-related YL1 band in unintentionally C-doped GaN and also attributed to passivation of the C_N acceptors by hydrogen released from unknown defects. In this case, the formation of the C_NH_i complexes was confirmed by the observation of the rising BL2 band associated with these complexes. At T_{ann} > 900 °C, both the YL_{Be} and YL1 intensities were restored, which was explained by the removal of hydrogen from the samples. Experimental results were compared to the first principles calculations of complex dissociation and hydrogen diffusion paths in GaN.

* E-mail: mreshchi@vcu.edu

I. INTRODUCTION

Hydrogen plays a critical role in GaN processing, affecting devices' optical and electrical properties by creating complexes with impurities, leading to their passivation.[1] Annealing stands as a widely utilized technique for defect activation. The most important example emphasizes the role of hydrogen in *p*-type GaN grown by metalorganic chemical vapor deposition (MOCVD) and doped with Mg.

The as-grown GaN:Mg has high resistivity (~10^6 Ωcm) because H (an abundant by-product in MOCVD) passivates Mg by forming inactive Mg-H complexes.[2,3,4,5] Nakamura et al.[2,3] has discovered that the high-resistivity GaN:Mg converts into conductive *p*-type (~2 Ωcm) after annealing in N_2 ambient at temperatures (T_{ann}) above 600-700 °C. Annealing of this high-conductivity material in the NH_3 ambient at T_{ann} > 600 °C converts it back to the high-resistivity state. These reversible processes were explained by the dissociation of the Mg-H complexes that activated the Mg acceptors and by the passivation of Mg with H, respectively. It was proposed that the NH_3 dissociates into hydrogen atoms at the GaN surface at T > 400 °C, which diffuse into the bulk and form the Mg-H complexes. Nakamura et al.[3] also noticed a correlation between the hole conductivity and room-temperature photoluminescence (PL) features. Namely, the Mg-related blue luminescence (BL_{Mg}) band with a maximum at 2.8 eV was stronger in conductive *p*-type and was diminished by hydrogen passivation. On the other hand, the defect-related red luminescence (RL_{Mg}) band correlated with the presence of hydrogen.

Later, the passivation of Mg acceptors by H and their activation by annealing in hydrogen-free ambient were studied and explained in more detail. Early first-principles calculations predicted that hydrogen is in the 1+ charge state when the Fermi level is lower than 2.2-2.4 eV above the valence band maximum (VBM), and it is negatively charged when the Fermi level is

closer to the conduction band.[6,7] These calculations also showed that the barrier for diffusion of H^+ in the *c* direction is 0.94 eV and that for H^- is 1.99 eV.[7] These predictions agree with experimental results, according to which hydrogen diffuses readily in *p*-type GaN at $T > 600$ °C, while no diffusion could be observed in *n*-type GaN up to 1050 °C.[8,9,10] More recent calculations revealed that the –/+ transition level of hydrogen is at 3.0 eV above the VBM,[11] the barrier for the H^+ diffusion along the *c* axis is 1.08 eV, and the barrier for the dissociation of the $Mg_{Ga}H_i$ complex is 1.88 eV[12] or 1.3 eV.[11] In addition to the complex dissociation and H^+ diffusion barriers, there is a barrier for hydrogen to leave a GaN sample. Myers *et al*.[13] estimated the activation energy for recombinative desorption of hydrogen to be at least 2 eV; i.e., the release of hydrogen from GaN is limited by a surface permeation barrier, not by dissociation or diffusion. At least 700 °C is needed to remove hydrogen from the sample.[11,13] The presence of the Mg-H complexes in GaN:Mg grown by MOCVD and their dissociation after thermal annealing was also confirmed with infrared absorption experiments where local vibrational modes of the Mg-H and Mg-D complexes were identified.[14,15,16]

The effects of H on defects other than Mg in GaN and the effect of hydrogen on PL are less studied. We have shown earlier that the C_N acceptor readily forms complexes with hydrogen (C_NH_i) in undoped or C-doped high-resistivity GaN.[11,17] The C_N and C_NH_i defects are revealed in PL experiments as the yellow luminescence (YL1) band with a maximum at 2.17 eV and the blue luminescence (BL2) band with a maximum at 3.0 eV, respectively. An interesting feature in PL is that under UV light at low temperatures (< 80 K), the BL2 band bleaches (i.e., its intensity decreases with time under contentious laser illumination at a fixed temperature), and simultaneously, the YL1 band rises. This unique transformation of the PL spectrum was explained by the dissociation of the C_NH_i complex as a result of a photo-induced defect reaction.[11]

In this work, we examined the effects of annealing in N_2 and N_2+H_2 ambients on PL properties of acceptors in GaN, with emphasis on the Be_{Ga} and C_N acceptors. The changes in PL intensities upon annealing are attributed to the passivation of acceptors with H and their activation.

II. METHODS

A. Experimental Details

We studied the effect of thermal annealing on PL properties in several Be-doped GaN samples grown by MOCVD (Table I). The ~500 nm-thick GaN:Be layers were grown under nitrogen-rich conditions on ~3 μm-thick unintentionally doped GaN on c-plane sapphire substrates.[18] In sample R134, the GaN:Be layer was grown directly on sapphire. Beryllium acetylacetonate ($Be(acac)_2$) from Strem Chemicals was used as a Be precursor. Immediately after GaN:Be growth at 970 °C,

Table I. Parameters of MOCVD-grown GaN:Be samples before and after annealing in N_2 ambient at T_{ann} = 750 °C. Peak PL intensities at P_{exc} = 0.13 W/cm^2 and T = 18 K are given in relative units.

Sample	Be flow (nmol/min)	[Be] 10^{18} cm^{-3}	Type	PL intensity before/after annealing at 750 °C		
				YL_{Be}	UVL_{Be}	UVL_{Mg}
R26	1000	0.8	*n*	12/13	<0.01	0.35/0.35
R40	3010	40	*p*	11/11	0.7/0.9	<0.01
R41	3010	20	SI	8.1/7.9 [a)]	0.06/0.06 [a)]	<0.01 [a)]
R57	455	3	SI	7.2/4.6	0.2/0.2	0.35/0.27
R60	80	<0.1	SI	0.55/0.24	<0.1	14/11
R62	137	<0.1	SI	1.3/0.8	<0.1	1.5/0.8
R68	455	1	SI	5.3/1.2	<0.1	0.07/0.06
R69	455	~1 [b)]	SI	5.9/1.3	<0.1	0.42/0.36
R87	910	4	SI	7.2/4.8	2.8/3.3	<0.1
R96	910	3	SI	4.9/0.6	0.1/0.1	0.4/0.34
R98	910	~3 [b)]	SI	3.5/0.5	0.1/0.1	0.77/0.52
R134	910	~3 [b)]	SI	5.8/4.4	1.9/2.5	<0.1

[a)] PL data for sample R41 are given at T = 80 K before and after annealing in vacuum at T_{ann} = 400 °C.

[b)] For these samples the approximate values of [Be] are given based on comparison with the SIMS data for samples grown in the same conditions.

the material was annealed *in situ* under flowing N_2 at 500 Torr and 750 °C for 30 min without removing from the growth chamber. Samples R41 and R69 were not annealed *in situ*. The concentration of Be was measured by secondary ion mass spectrometry (SIMS) with a detection limit of about 10^{17} cm^{-3} for [Be]. Sample R26 is conductive *n*-type with a room-temperature concentration of electrons of about 10^{18} cm^{-3}.[19] Temperature-dependent Hall effect measurements were conducted for sample R40 and confirmed that it is *p*-type with a concentration of free holes of about 10^{13} cm^{-3} at room temperature.[20] Hot-probe measurements indicated *p*-type for samples R40, R41, and R87. From PL measurements, all the samples in Table I, except for R26, behaved as semi-insulating (SI) semiconductors. Namely, PL quenching (i.e., decreasing PL intensity with increasing temperature) occurred by the abrupt and tunable mechanism.[21]

The effect of thermal annealing on C_N acceptors was studied in undoped GaN sample s1587. This sample was investigated before with an emphasis on the BL2 band attributed to the C_NH_i complex.[11] From the SIMS measurements, the C, H, and O concentrations in this sample are 1.7×10^{17}, 3.0×10^{17}, and 1.3×10^{17} cm^{-3}, respectively. The room-temperature concentration of free electrons is $n = 2.6\times10^{16}$ cm^{-3} from the Hall-effect measurements. From detailed PL studies, we concluded that concentrations of the isolated C_N acceptors and C_NH_i complexes are 0.7×10^{17} and 1×10^{17} cm^{-3}, respectively, in this sample before subjecting it to thermal annealing or intense UV light exposure at low temperatures.[11]

Steady-state PL was excited with a HeCd laser at 325 nm, dispersed by a 1200 rules/mm grating in a 0.3-m monochromator, and detected by a Peltier-cooled photomultiplier tube and a photon-counting module. A closed-cycle optical cryostat was used for temperatures between 18 and 320 K, and a high-temperature optical cryostat was used for temperatures between 80 and 673

K. The as-measured PL spectra were corrected for the measurement system's spectral response, and PL intensity was additionally multiplied by λ^3, where λ is the light wavelength, to present the PL spectra in units proportional to the number of emitted photons as a function of photon energy.[17,22] All the samples were measured in identical conditions, and standards were used to verify the reproducibility of PL spectra.

The GaN:Be samples in Table I were annealed for one hour in N_2 ambient at T_{ann} = 750 °C. The peak intensities of the YL_{Be} (at 2.15 eV), UVL_{Be} (3.38 eV) and UVL_{Mg} (3.27 eV) bands before and after this annealing are shown in the last three columns. Four samples (R62, R68, R96, and R98) were annealed for one hour in a wide range of T_{ann} (between 300 and 1000 °C). For this, 2-inch wafers were cut into 5×5 mm squares, and for each piece, PL at 18 K was studied before and after annealing at a particular temperature. Several samples (including R69 in Table I) were also annealed in the H_2+N_2 ambient at T_{ann} = 750 °C to explore possible passivation with H in these conditions. Finally, samples R41, R62, R68, R69, R87, and R98 were also subjected to isochronal annealing (30-min steps) in a high-temperature optical cryostat, in a vacuum, and at temperatures up to 400 °C. PL in these samples was measured at 80 K before and after each annealing step. Details about the annealing of undoped GaN sample s1587 can be found in Ref. 11.

B. Computational Details

Ab initio modeling of the dissociation of $Be_{Ga}H_i$, $Mg_{Ga}H_i$, and C_NH_i complexes was performed using the Heyd-Scuseria-Ernzerhof (HSE) hybrid functional[23] as implemented in the VASP code. The HSE functional was tuned to fulfill the generalized Koopmans' condition for the Be_{Ga}, Mg_{Ga}, and C_N acceptors separately. Details of the supercell error corrections and tuning procedures are described in Ref. 24. The resulting HSE parametrizations were obtained with values of the fraction

of the exact exchange α of 0.226, 0.274, and 0.268 for the deep states of Be_{Ga}, Mg_{Ga}, and C_N acceptors, respectively (the range separation parameter was kept at 0.2 $Å^{-1}$). All calculations were performed using the nudged elastic band method in 300-atom hexagonal supercells at the Γ-point, with plane-wave energy cutoffs of 500 eV. All defect atomic structures were relaxed using HSE to minimize the forces to 0.05 eV/Å or less. The calculations were performed for the neutral charge state of the acceptor-hydrogen complexes, which is the lowest energy charge state for most Fermi energies.

III. EXPERIMENTAL RESULTS

A. Passivation of the Be_{Ga} acceptors in GaN

In Be-doped GaN samples grown by MOCVD, in addition to the excitonic near-band-edge (NBE) emission with a maximum at about 3.47 eV, three defect-related PL bands are commonly observed (Fig. 1). These are the YL_{Be} band with a maximum at 2.15 eV (attributed to a polaronic state of the Be_{Ga} acceptor),[25] the UVL_{Be} band with the strongest peak at 3.38 eV followed by a few LO

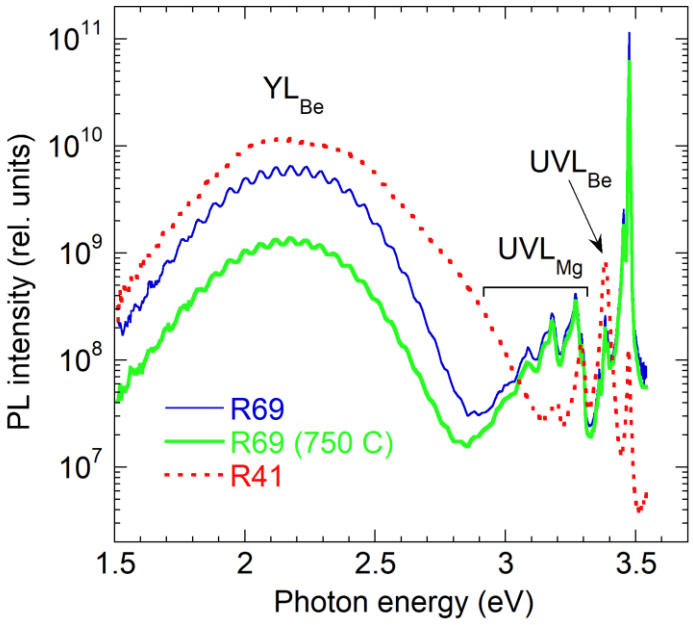

Fig. 1. PL spectra at $T = 18$ K and $P_{exc} = 0.13$ W/cm^2 from representative GaN:Be samples not annealed *in situ*.

phonon replicas (attributed to the shallow state of the $Be_{Ga}O_NBe_{Ga}$ complex),[26] and the UVL_{Mg} band with the strongest peak at 3.27 eV followed by LO phonon replicas (attributed to the Mg_{Ga} acceptor).[27] The latter is caused by contamination of GaN with Mg during MOCVD growth, typically with concentrations below 10^{16} cm^{-3}. Assuming that Be_{Ga} and Mg_{Ga} are similarly passivated during the growth,[28] and their activation requires annealing, the samples were annealed *in situ* under flowing N_2 at 500 Torr and 750 °C for 30 min without removing from the growth chamber. However, three samples (R39, R41, and R69) were not annealed, and no significant difference was observed in their PL behavior between the annealed and not annealed GaN:Be samples. This may indicate that Be-related acceptors in as-grown GaN:Be were not passivated with H or the passivation was insignificant in contrast to the Mg passivation in *p*-type GaN:Mg.

Figure 2 shows the dependences of the YL_{Be}, UVL_{Mg} and NBE intensities on T_{ann} for four GaN:Be samples with [Be] = (1-3)×10^{18} cm^{-3} annealed for one hour in N_2 ambient. An increase in the UVL_{Mg} intensity begins at $T_{ann} \approx 700$ °C and can be attributed to the activation of the Mg_{Ga} acceptors, in agreement with earlier findings.[2,3] The most interesting behavior was observed for the YL_{Be} band: its intensity abruptly decreased at T_{ann} = 350-400 °C. The YL_{Be} drop was measured more carefully when annealing was conducted in a vacuum using a high-temperature optical cryostat (Fig. 3). The YL_{Be} intensity remained reduced up to 800 °C, after which it increased and approached the initial value. Note that very similar behavior was observed both for GaN:Be samples annealed *in situ* under flowing N_2 at 750 °C and for samples cooled down after the growth without additional annealing. There was no change of PL intensity in *n*-type GaN:Be (sample R26) and in samples with high concentrations of Be (R40 and R41). For other samples, the YL_{Be} intensity drop was always observed at $T_{ann} > 350$ °C, but the magnitude of the drop was different in different samples (Table I).

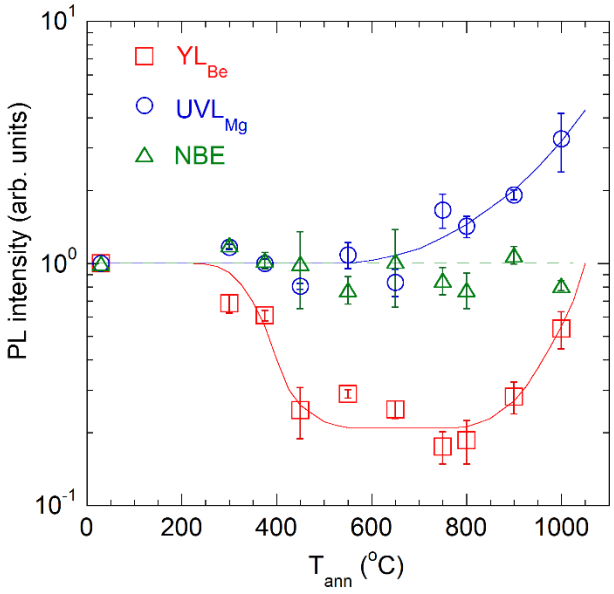

Fig. 2. PL intensities of the YL_{Be}, UVL_{Mg} and NBE bands at T = 18 K as a function of annealing temperature for one hour in N_2 ambient. The symbols show mean values for four GaN:Be samples (R68, R69, R96, R98), and the error bars represent the standard deviation of the mean. The lines are guides for the eyes.

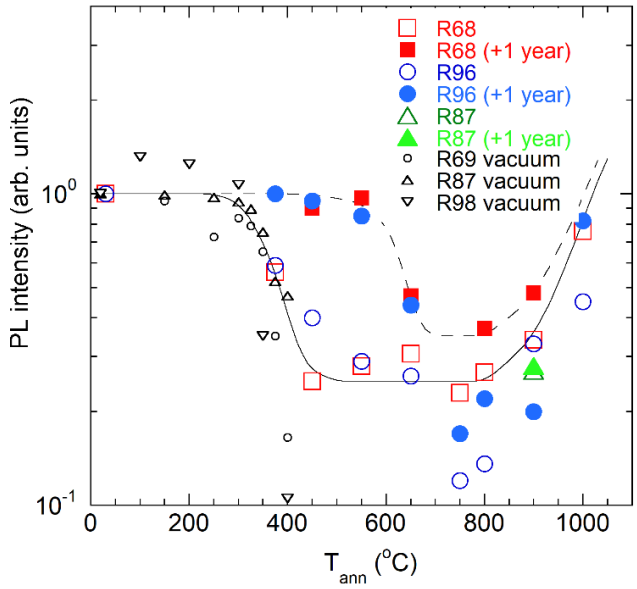

Fig. 3. Low-temperature PL intensities of the YL_{Be} band in selected GaN:Be samples as a function of annealing temperature for one hour in N_2 ambient (large symbols) and for 30 min in vacuum (small symbols). The empty symbols show the PL intensities one day after the annealing, and the filled symbols show the PL intensities after one year. The lines are guides for the eyes.

At first glance, a simple explanation for the YL_{Be} intensity drop would be the passivation of the Be_{Ga} acceptors with hydrogen. Indeed, it is observed only in semi-insulating or *p*-type GaN:Be samples where H^+ ions are mobile at moderate temperatures. In principle, gallium and nitrogen vacancies (V_{Ga} and V_N) could also be mobile at $T_{ann} \approx 400$ °C in GaN.[7,29,30,31,32] However, as will be shown in Sec. V, passivation of the Be_{Ga} by the vacancies is not expected in our MOCVD-grown GaN:Be samples.

At $T_{ann} = 1000$ °C, the YL_{Be} intensity is restored, which can be explained by removing H from GaN samples. To verify this assumption, we annealed sample R68 at 750 °C after it was annealed at 1000 °C, and the YL_{Be} intensity did not change. We also tried hydrogenating the Be_{Ga} acceptors by annealing samples at 750 °C in the N_2+H_2 ambient. However, in contrast to the successful hydrogenation of the C_N acceptors in these conditions,[11] annealing of GaN:Be samples (as-grown or annealed in N_2 at $T_{ann} = 300$-800 °C) in the N_2+H_2 ambient caused the same effect as annealing in N_2 at 750 °C.

The drop in the YL_{Be} intensity is not permanent. After a year of storage at room temperature in air ambient conditions, at least for samples annealed at $T_{ann} < 600$ °C, the YL_{Be} intensity was completely restored (Fig. 3), which was also accompanied by reproduced shapes and intensities of the UVL_{Mg} and NBE bands. This YL_{Be} restoration is slow (at the scale of months) and apparently not activated by temperature. More discussion of these processes will be presented in Sec. V.

B. Passivation of the C_N acceptors in GaN

Earlier, we studied the effect of thermal annealing on the BL2 band, which is caused by the C_NH_i complexes in GaN.[11] The effect of the annealing on the YL1 band, which is attributed to the C_N acceptors, was overlooked in that work. The evolution of the YL1 intensity with T_{ann} is shown in

Fig. 4. Very similar to the YL_{Be} band in GaN:Be, the YL1 intensity drops at $T_{ann} \approx 350$ °C and restores at $T_{ann} > 900$ °C. Note that these annealing experiments were done in "face-to-face" geometry when the GaN surface was covered by another GaN sample. In these conditions, the BL2 band also started disappearing only at $T_{ann} > 900$ °C because the contact with another GaN sample obstructed the evaporation of hydrogen from the surface.[11]

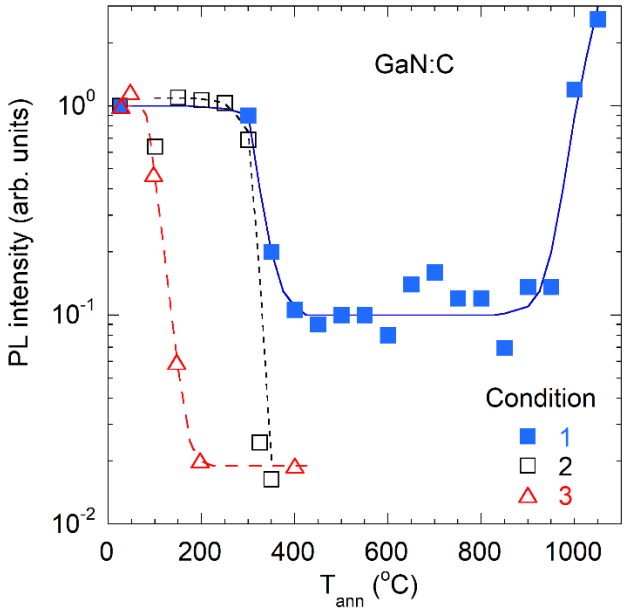

Fig. 4. The YL1 intensity in undoped GaN (sample s1587) as a function of annealing temperature for one hour in N_2 ambient (solid squares) and for 30 min in vacuum (empty symbols). The solid squares (1) show changes in the YL1 intensity at 18 K in separate 5×5 mm pieces after annealing them for one hour in N_2 ambient at selected T_{ann} (between 350 and 1000 °C. The empty squares (2) show the evolution of the YL1 intensity in another piece of as-grown GaN sample s1587 after consecutive 30-min annealing steps in a vacuum at T_{ann} = 100-350 °C. Then the YL1 band was restored at T = 80 K by extended (2 hours) exposure to high-intensity UV light. The empty triangles (3) show the annealing-related evolution of the YL1 intensity after this UV exposure. The lines are guides for the eyes.

An as-grown GaN sample (s1587) was annealed in a vacuum at 400 °C for 30 min, and PL spectra at 80 K before and after the *in situ* annealing were compared (Fig. 5). To avoid bleaching of the BL2 band due to dissociation of the C_NH_i complexes, the PL measurements were carried out

at very low excitation intensity (10^{-4} W/cm^2). After the annealing at 400 °C, the YL1 intensity dropped by two orders of magnitude. Then, the sample was subjected to high-intensity UV light (325 nm, 0.13 W/cm^2) irradiation at T = 80 K for one hour. This resulted in almost complete restoration of the YL1 band (Fig. 5) due to photo-induced dissociation of the C_NH_i complexes.

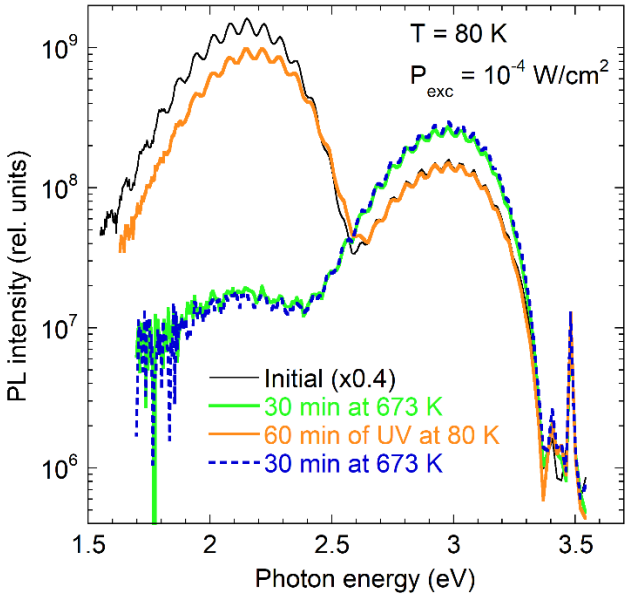

Fig. 5. Evolution of PL spectrum in GaN (sample s1587) at 80 K as a result of *in situ* annealing for 30 min at 400 °C, the following exposure of the sample to high-intensity (0.13 W/cm^2) UV light for 1 hour at 80 K, and additional *in situ* annealing for 30 min at 400 °C.

Next, 30-minute-long *in situ* annealing steps in a vacuum were repeated. The evolution of the PL spectrum at T = 80 K and P_{exc} = 10^{-4} W/cm^2 is shown in Fig. 6. In these conditions, the drop of the YL1 band began already at T_{ann} =100 °C. Simultaneously, the BL2 band intensity increased. The above results indicate that while the passivation of the C_N acceptors by hydrogen begins at ~350 °C in as-grown GaN, it occurs at much lower temperatures (100-150 °C) if the YL1 band is restored by photo-induced defect reaction at low temperatures. The explanations for these effects will be given in Sec. V.

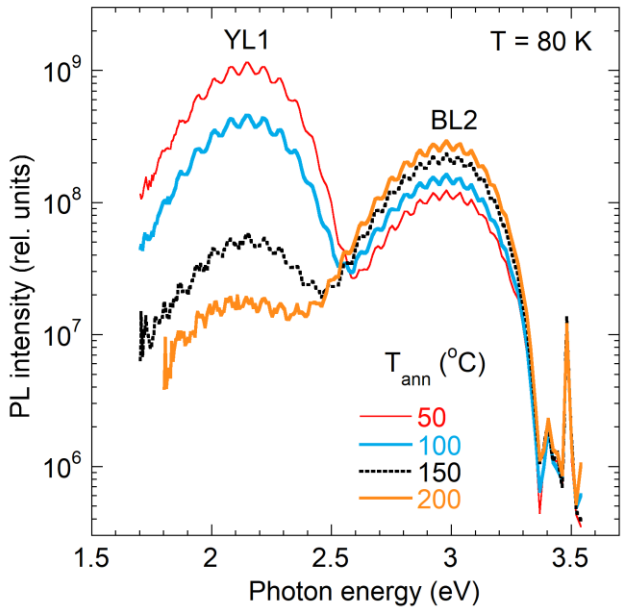

Fig. 6. Evolution of PL spectrum in undoped GaN (sample s1587) at 80 K after consecutive 30-min-long steps of *in situ* annealing at indicated temperatures.

IV. COMPUTATIONAL RESULTS

The initial acceptor-hydrogen complex geometries were those of the respective lowest energy. These are different for the complexes considered here. For the $Be_{Ga}H_i$ and $Mg_{Ga}H_i$ complexes, these are where the H_i occupies a bond-center interstitial site nearest an acceptor (Fig. 7(a)). For the C_NH_i, the lowest energy geometry is where H_i is occupying the carbon anti-bonding site (AB_C), a C-H bond length is 1.1 Å along the direction opposite the C-Ga bond (Fig. 7(b)). The bond center C_NH_i geometry is 0.5 eV higher in energy. In contrast, the H_i acceptor anti-bonding sites for $Be_{Ga}H_i$ and $Mg_{Ga}H_i$ complexes are 2.9 and 3.1 eV higher in energy than the respective bond-center sites. The hydrogen atom was moved to the nearest anti-bonding nitrogen (AB_{N1}) site (Fig. 7), as the first step in the dissociation process, then to the next AB_{N2} site further along the wurtzite *c* axis, and the next stable AB_{N3} site to model hydrogen diffusion.

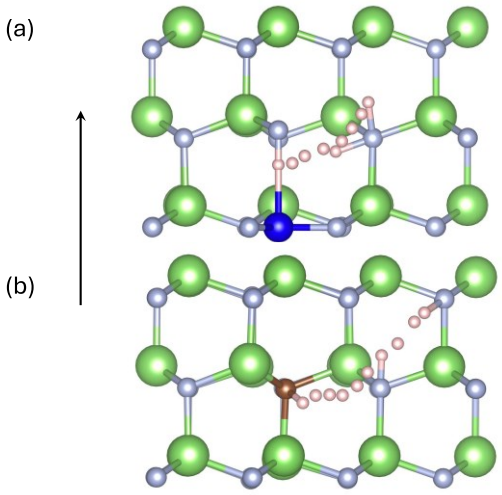

Fig. 7. Dissociation pathways of (a) $Be(Mg)_{Ga}H_i$ and (b) C_NH_i complexes in GaN lattice.

The resulting energy barriers along these dissociation paths for the $Be_{Ga}H_i$, $Mg_{Ga}H_i$, and C_NH_i complexes are shown in Fig. 8, where the defect total energies are plotted as a function of the hydrogen displacement. Since the defect complexes consist of different chemical species, their total energies cannot be compared directly. In Fig. 8, defect total energies are plotted bringing the total energies of the dissociated complexes (i.e., an isolated acceptor and hydrogen at the most distant site) to the same value. Overall, Fig. 8 shows that potential barriers for the acceptor-hydrogen association are about 2-3 times lower than for the complex dissociation. Furthermore, the complex formation barriers between an isolated acceptor and an interstitial hydrogen are similar 0.6-0.7 eV for all three complexes. In contrast, there is a significant difference in the dissociation and binding energies among the complexes. While the dissociation barriers of C_NH_i and $Mg_{Ga}H_i$ are 1.3 and 1.5 eV, respectively, the dissociation barrier of the $Be_{Ga}H_i$ complex is 2.2 eV. The slope of the potential curves of the dissociated hydrogen towards the acceptors also indicates the presence of the long-range Coulomb attraction between an acceptor and the dissociated hydrogen. An additional relatively low diffusion barrier of ~0.5 eV is predicted to

move hydrogen farther away from the C_N acceptor. This barrier is higher (~0.8 eV) for Be_{Ga} and Mg_{Ga}.

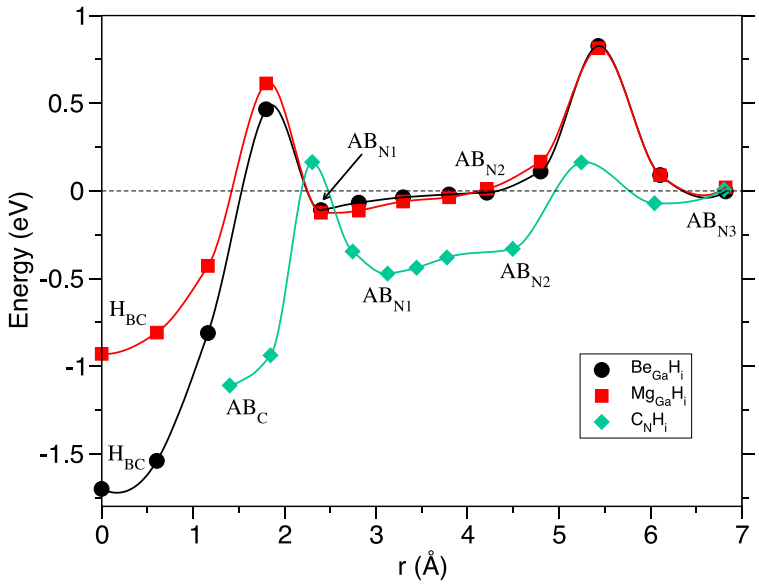

Fig. 8. Total energies of $Be_{Ga}H_i$, $Mg_{Ga}H_i$, and C_NH_i complexes along the hydrogen pathways shown in Fig. 7.

Interstitial hydrogen was suggested to be positively charged and mobile in GaN when the Fermi level is lower than 3.0 eV above the VBM.[11] The lowest energy charge state of H_i is singly negative in *n*-type GaN for the Fermi levels above ~3 eV, which significantly reduces its mobility. Our HSE calculations suggest that if interstitial hydrogen is available in *p*-type and high resistivity samples, it should readily bind to the isolated negatively charged acceptors at room temperature due to the low complex association barriers. Dissociation of acceptor-hydrogen complexes can be expected for annealing at moderate temperatures. However, a relatively flat potential landscape for H_i around an acceptor, Coulomb attraction between H_i^+ and a negatively charged acceptor, and low association barrier suggest that the dissociated complexes will quickly re-bind during the sample cooling following annealing. Lower energies of interstitial H_i around C_N suggest that C_NH_i complex is quicker to bind than $Be_{Ga}H_i$ and $Mg_{Ga}H_i$. Therefore, it is expected that annealing

experiments followed by the low-temperature PL measurements cannot extract acceptor-hydrogen dissociation energies. Rather, hydrogen would have to be annealed out of the sample in order to activate acceptor-related PL bands. Further analysis of the acceptor-hydrogen complex dissociation/association energetics is given in Sec. V.

V. DISCUSSION

The isochronal annealing process leading to the dissociation of H-containing complexes can be described as [32,33]

$$N_{i+1} = N_\infty + \left(N_i - N_\infty\right)\exp\left[t_{ann}\nu\exp\left(-\frac{E_A}{kT_{ann}^i}\right)\right], \quad (1)$$

where i denotes the annealing step, t_{ann} is the annealing time, ν is the dissociation attempt frequency (can be taken as the phonon frequency, about 10^{13} s^{-1}), and E_A is the activation energy of the dissociation. Figure 9 shows examples of isochronal annealing in a vacuum, where relative PL intensity is fitted with Eq. (1) in the assumption that the PL intensity is proportional to the concentration of the isolated Be_{Ga} or C_N defects.

For a rough estimate, the relation between E_A and the critical temperature at which the dissociation begins can be found from

$$w = t_{ann}\nu\exp\left(-\frac{E_A}{kT_{ann}}\right) \approx 1. \quad (2)$$

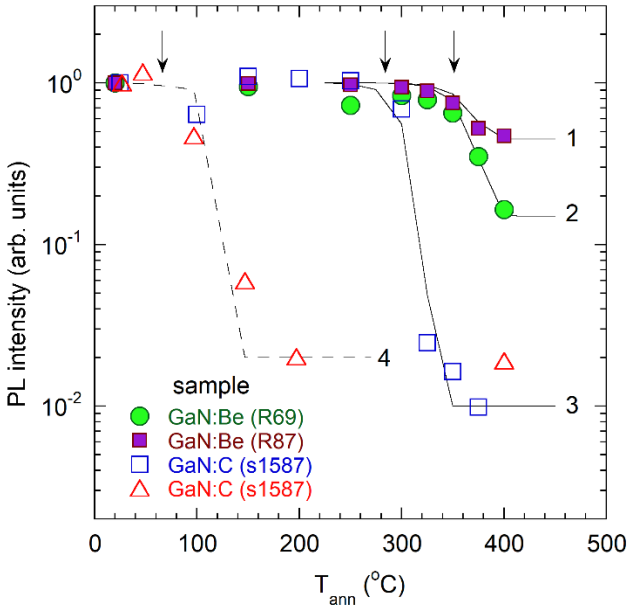

Fig. 9. Evolution of the YL_{Be} intensity in GaN:Be (filled symbols) and YL1 intensity in undoped GaN (empty symbols) as a function of annealing temperature for 30 min in a vacuum. The experimental data are taken from Figs. 2 and 3. The lines are calculated using Eq. (1) with the following parameters: t_{ann} = 1800 s, v = 10^{13} s^{-1}, E_A = 2.0 eV (1,2), 1.8 eV (3), and 1.1 eV (4), N_∞/N_0 = 0.45 (1), 0.15 (2), 0.01 (3) and 0.02 (4). The arrows show the critical temperatures obtained from Eq. (2) for E_A = 1.1, 1.8, and 2.0 eV.

Figure 10 shows the calculated $E_A(T_{ann})$ dependences for selected t_{ann}. Note that if the formation of the H-containing complexes requires overcoming a potential barrier E_A, the probability of the complex formation will also be described with Eq. (2).

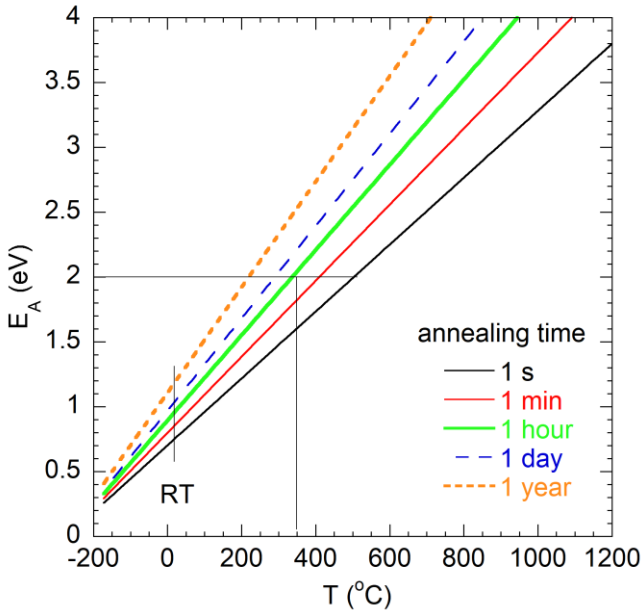

Fig. 10. The dependence of the dissociation energy E_A on annealing temperature for selected annealing times calculated with Eq. (2).

According to Fig. 10, $T_{ann} \approx 900$ °C, at which an increase of the YL_{Be} and YL1 intensities begins, corresponds to $E_A = 3.8$ eV. This is significantly larger than the acceptor-hydrogen dissociation barriers predicted by HSE calculations, 1.3 and 2.2 eV for $Be_{Ga}H_i$ and C_NH_i complexes, respectively. According to a detailed study of the dissociation of H-containing complexes in Mg-doped GaN,[13] a large portion of hydrogen may remain in the sample after annealing temperatures up to 900 °C because of a high surface permeation barrier. This is also consistent with our earlier findings showing that removal of H from undoped GaN samples occurs at critical temperatures of ~650 and 1000 °C, respectively, for the open-surface and face-to-face geometries of the annealing, which revealed the activation energies of 3.0 and 4.2 eV, respectively.[11] The estimates for the YL1 band in the current work agree with the results reported in Ref. 11 (for the sample annealed in the face-to-face geometry). The GaN:Be samples were annealed in the open-surface geometry, and $E_A = 3.8$ eV for them seemingly contradicts the smaller

value (3.0 eV) obtained for the BL2 band in undoped GaN.[11] However, this apparent disagreement can be explained by different near-surface band bending in the GaN:Be and undoped GaN samples. In high-resistivity *n*-type GaN samples studied in Ref. 11, an upward band bending is expected, which favors the extraction of positively charged hydrogen atoms. In contrast, the near-surface band bending in the studied GaN:Be samples (*p*-type and semi-insulating) is most likely downward, as it is typical for *p*-type semiconductors. The related electric field repels H^+ ions, and higher temperatures are needed to remove hydrogen from GaN:Be samples. We conclude that at T_{ann} < 900 °C hydrogen remains in GaN samples and inevitably forms H-containing complexes after cooling down to room temperature.

It can be seen from Figs. 9 and 10 that the critical temperatures T_{ann} = 350-400 °C at which PL intensities of the C_N-related YL1 and Be_{Ga}-related YL_{Be} bands significantly decrease during 30-60 min of annealing correspond to E_A = 1.8-2.0 eV. Note that finding E_A from the critical T_{ann} is more accurate than finding it from the slope in the Arrhenius plot dependence because the latter may be abnormally small if the number of experimental points is insufficient or some other processes occur simultaneously with the dissociation. The obtained activation energies (E_A = 1.8-2.0 eV) cannot be attributed to the barriers for complex formation (the calculated values are 0.6-0.7 eV). We suggest that in as-grown GaN, hydrogen is trapped at some unknown defects (nonradiative or electrically inactive), and the dissociation energy of the related H-containing complexes is about 1.8-2.0 eV. The origin of these defects, called X hereafter, is unknown (they may be point or extended defects). These defects trap a significant portion of hydrogen atoms after the growth.

In situ annealing of GaN:Be samples at 750 °C in N_2 ambient does not remove hydrogen from the samples (higher than 900 °C temperature is required for this), and a significant portion of

hydrogen atoms remains trapped at the X defects. Unlike the case of undoped GaN, where both the C_N and C_NH_i defects are radiative, we cannot say if the Be_{Ga} acceptors in GaN:Be samples are all activated or if some of them are passivated with H after the growth and cooling down to room temperature. However, the fact that additional annealing at T_{ann} = 400-800 °C passivates a significant portion of the isolated Be_{Ga} defects (up to 90% for samples demonstrating the reduction of the YL_{Be} intensity by a factor of 10), suggests that in as-grown GaN:Be samples most Be_{Ga} acceptors are free of hydrogen and that H_i^+ are not readily available, but are rather bound to some other defects.

A remarkable feature is that at least for T_{ann} = 400-600 °C the Be_{Ga} acceptors are activated back after storing them for one year at room temperature (Fig. 3). If the restoration was thermally activated, the barrier for this process would be about 1.2 eV from Fig. 10. Simple rate-equations models with two types of defects (a radiative acceptor and the defect X that may trap and release hydrogen) cannot explain the observed complex behavior of PL under different annealing and storing conditions. More information is needed to explain the results consistently.

It is important to notice that the above situation is similar to that in Mg-doped *p*-type GaN. Myers et al.[13] emphasized that electrical activation of Mg acceptors occurs at T_{ann} = 500-600 °C, while practically all hydrogen atoms remain in GaN:Mg samples after annealing at these temperatures. This means that after MOCVD growth of GaN:Mg and cooling down to room temperature, most of the hydrogen atoms are bound to Mg_{Ga} acceptors (X centers in case of GaN:Be), whereas after annealing at 500-600 °C hydrogen atoms become bound to unknown defects (Be_{Ga} acceptors in case of GaN:Be). Based on our findings for MOCVD-grown GaN:Be, we expect that after a long time of storage at room temperature (about a year for GaN:Be), Mg_{Ga}

acceptors may also become passivated again. This can detrimentally affect the performance and longevity of GaN-based devices.

Let us now discuss the abrupt decrease of the YL1 intensity in GaN:C samples at $T_{ann} \approx 100$ °C after it is restored by UV light (Fig. 4). According to Figs. 3 and 4, this process corresponds to $E_A = 1.1$ eV. This value also agrees with the fact that it takes several days at room temperature to fully restore the BL2 and YL1 intensities after the C_NH_i dissociation under intense UV illumination at low temperatures. We conclude that free H interstitials must overcome a barrier of about 1.1 eV to form the C_NH_i complexes and the estimated activation energy is slightly larger than the C_NH_i association energy of 0.7 eV predicted by theory (Sec. IV). We also obtain a migration barrier of about 0.5 eV (Fig. 8) to move a dissociated H_i to a more distant AB_{N3} site (Fig. 7). Previously, the barrier for H_i^+ migration in GaN, which involved bond-center sites, was theoretically predicted to be about 1.0 eV.[34] Careful analysis of PL spectra (such as shown in Fig. 5) indicates that after the photo-induced restoration, the YL1 band is blue-shifted by 30-40 meV as compared to its position in the as-grown sample. This shift can be explained by the Coulomb attraction between the C_N^- and H^+ ions located close to each other.

No passivation effects were observed in GaN:Be samples with a high concentration of Be ([Be] > 10^{19} cm^{-3} in samples R40 and R41). This can be explained by the assumption that the concentration of H is much smaller than that of Be, and the effects of passivation/activation remain unnoticed. From SIMS measurements, the concentrations of Be and H in the 200 nm near-surface layer of sample R40 are ~4×10^{19} and ~3×10^{18} cm^{-3}, respectively, where the latter is close to our H detection limit (1-2×10^{18} cm^{-3}) and could be caused by kick-on of the impurity atoms from the surface contaminations into the depth by the primary ion beam. This contrasts to Mg-doped GaN

grown by MOCVD, for which the concentration of hydrogen increases with Mg doping and is nearly equal to that of Mg.[35,36]

It is known that the V_{Ga} and V_N defects are also mobile in GaN at annealing temperatures explored in the current work. According to the literature data, the isolated V_{Ga} defects are mobile at T > 300-500 °C.[31,32,37] We expect that the isolated V_{Ga} defects are unlikely to remain in GaN after the growth, post-growth annealing, and cooling down because they either diffuse to the surface or preferentially form stable complexes with O_N donors that are omnipresent in GaN. The $V_{Ga}O_N$ complexes dissociate only at T > 1300 °C.[31,38] We also do not expect V_N defects in our MOCVD-grown GaN:Be because these samples were grown in N-rich conditions. The V_N and $Be_{Ga}V_N$ defects can be reliably identified in PL spectra from semi-insulating GaN.[39,40,41] Namely, the green luminescence (GL2) band at 2.33 eV is caused by the isolated V_N defect,[39,40] and the red luminescence (RL_{Be}) band with a maximum at 1.8 eV is caused by the $Be_{Ga}V_N$ complexes.[40,41] In MBE-grown GaN:Be, these PL bands appear and become very strong after annealing at 900 °C, apparently due to the abundant formation of nitrogen vacancies at such high temperatures in this material. However, we did not observe the GL2 and RL_{Be} bands in our GaN:Be samples grown by MOCVD in N-rich conditions, even in samples annealed at high temperatures.

We observed a significant reduction of the YL_{Be} band intensity with annealing (attributed to the passivation of the Be_{Ga} acceptors with H) but did not observe such an effect for the UVL_{Mg} and UVL_{Be} bands in the same GaN:Be samples. The UVL_{Mg} band is caused by the Mg_{Ga} acceptor. Its intensity slightly increased at T_{ann} > 800 °C (Fig. 2), which can be attributed to the dissociation of the $Mg_{Ga}H_i$ complexes and the removal of hydrogen from the samples. Note that these samples contained very low concentrations of Mg, below the detection limit of SIMS measurements. Thus, when Be_{Ga} and Mg_{Ga} acceptors are present, hydrogen preferably forms complexes with Be.

Similarly, Be_{Ga} acceptors win a competition for hydrogen in samples containing Be_{Ga} and C_N acceptors. Indeed, MOCVD-grown GaN:Be samples contain a significant amount of carbon impurities, which is confirmed by SIMS measurements and the presence of a weak C_N-related YL1 band in PL spectra of some GaN:Be samples. However, we never observed the C_NH_i-related BL2 band in these samples. All these experimental findings agree with theoretical predictions, according to which, the $Be_{Ga}H_i$ complexes are the most stable among the complexes containing Be, Mg, or C (Fig. 8).

The UVL_{Be} band with the strongest peak at 3.38 eV is attributed to the $Be_{Ga}O_NBe_{Ga}$ complex.[26] In contrast to the YL_{Be} band (which is always strong), its intensity is high only in semi-insulating or *p*-type GaN:Be samples with a relatively high concentration of Be. For as-grown MOCVD GaN:Be samples with high intensity of the UVL_{Be} band (R87 and R134), annealing for one hour in N_2 ambient at T_{ann} = 400-900 °C resulted in a modest increase of the UVL_{Be} intensity. In as-grown MOCVD GaN:Be samples with a very weak UVL_{Be} band (R96 and R98), the UVL_{Be} intensity started increasing at T_{ann} > 800 °C, and it increased by about an order of magnitude by T_{ann} = 1000 °C. These changes can be attributed to the removal of hydrogen from GaN:Be samples and partial activation of the $Be_{Ga}O_NBe_{Ga}$ defects. Interestingly, in MBE-grown GaN:Be samples the UVL_{Be} band appears after annealing at T_{ann} > 700 °C, and its intensity increases by orders of magnitude at 800 °C. Additional annealing in H_2 ambient at T_{ann} = 550 °C or in N_2+H_2 ambient at T_{ann} = 600-850 °C did not cause any significant changes in the UVL_{Be} intensity.

VI. CONCLUSIONS

Unusual behavior of PL was observed for the Be_{Ga}-related YL_{Be} band and C_N-related YL1 band in GaN (both PL bands have a maximum at ~2.15 eV). Namely, the low-temperature YL_{Be} and YL1

intensities dropped by up to 1-2 orders of magnitude after annealing in a vacuum or N_2 ambient at annealing temperatures between 350 and 800 °C. The drop was attributed to the passivation of these acceptors by hydrogen. The critical temperature of ~350 °C corresponds to a release of hydrogen trapped at unknown defects after overcoming a potential barrier of about 2 eV. At T_{ann} > 900 °C, hydrogen is removed from the samples, and the yellow bands' intensities are restored. The observed behavior of hydrogen and technologically important acceptors in GaN could help identify post-growth processing for acceptor activation, and help search for more efficient *p*-type dopants in nitrides.

Acknowledgments

The work at VCU and SUNY was partly supported by the National Science Foundation under grants DMR-2423874 and DMR-2423875, respectively. The theoretical calculations were performed at the VCU High Performance Research Computing (HPRC) core facility.

Conflict of Interest

The authors have no conflicts to disclose.

Data Availability Statement

The data supporting this study's findings are available from the corresponding author upon reasonable request.

Keywords

Photoluminescence, GaN, passivation, point defects, thermal annealing, semiconductors.

References

[1] S. J. Pearton, J. C. Zolper, R. J. Shul, and F. Ren, "GaN: Processing, defects, and devices", J. Appl. Phys. **86**, 1-78 (1999)

[2] S. Nakamura, T. Mukai, M. Senoh, and N. Iwasa, "Thermal annealing effects on p-type Mg-doped GaN films", Jpn. J. Appl. Phys. **31**, Pt. 2, L139-L142 (1992).

[3] S. Nakamura, N. Iwasa, M. Senoh, and T. Mukai, "Hole compensation mechanism of p-type GaN films", Jpn. J. Appl. Phys. **31**, Pt. 2, 1258-1266 (1992).

[4] W. Gotz, N. M. Johnson, J. Walker, D. P. Bour, and R. A. Street, "Hydrogen passivation of Mg acceptors in GaN grown by metalorganic chemical vapor deposition", Appl. Phys. Lett. **67**, 2666-2668 (1995).

[5] S. J. Pearton, S. Bendi, K. S. Jones, V. Krishnamoorthy, R. G. Wilson, F. Ren, R. F. Karlicek, Jr., and R. A. Stall, "Reactivation of acceptors and trapping of hydrogen in GaN/InGaN double heterostructures", Appl. Phys. Lett. **69**, 1879-1881 (1996).

[6] J. Neugebauer and C. G. Van de Walle, "Hydrogen in GaN: Novel Aspects of a Common Impurity" Phys. Rev. Lett. **75**, 4452-4455 (1995).

[7] S. Limpijumnong and C. G. Van de Walle, "Stability, diffusivity, and vibrational properties of monoatomic and molecular hydrogen in wurtzite GaN", Phys. Rev. B **68**, 235203 (2003).

[8] W. Gotz, N. M. Johnson, J. Walker, D. P. Bour, and R. A. Street, "Activation of acceptors in Mg-doped GaN grown by metalorganic chemical vapor deposition", Appl. Phys. Lett. **68**, 667-669 (1996).

[9] R. Czernecki, E. Grzanka, R. Jakiela, S. Grzanka, C. Skierbiszewski, H. Turski, P. Perlin, T. Suski, K. Donimirski, and M. Leszczynski, "Hydrogen diffusion in GaN:Mg and GaN:Si", J. Alloys and Compounds **747**, 354-358 (2018).

[10] M. A. Reshchikov, D. O. Demchenko, D. Ye, O. Andrieiev, M. Vorobiov, K. Grabianska, M. Zajac, P. Nita, M. Iwinska, M. Bockowski, B. McEwen, and F. Shahedipour-Sandvik, "The effect of annealing on photoluminescence from defects in ammonothermal GaN", J. Appl. Phys. **131**, 035704 (2022).

[11] M. A. Reshchikov, O. Andrieiev, M. Vorobiov, B. McEwen, F. Shahedipour-Sandvik, D. Ye, and D. O. Demchenko, "Stability of the C_NH_i complex and the BL2 luminescence band in GaN", Phys. Stat. Sol. (b) **258**, 2100392 (2021).

[12] J.-S. Park and K. J. Chang, "Diffusion and stability of hydrogen in Mg-doped GaN: A density functional study", Appl. Phys. Express **5**, 065601 (2012).

[13] S. M. Myers, A. F. Wright, G. A. Petersen, W. R. Wampler, C. H. Seager, M. H. Crawford, and J. Han, "Diffusion, release, and uptake of hydrogen in magnesium-doped gallium nitride: Theory and experiment", J. Appl. Phys. **89**, 3195-3202 (2001).

[14] W. Gotz, N. M. Johnson, D. P. Bour, M. D. McCluskey, and E. E. Haller, "Local vibrational modes of the Mg-H acceptor complex in GaN", Appl. Phys. Lett. **69**, 3725-3727 (1996).

[15] A. Hoffmann, A. Kaschner, and C. Thomsen, "Local vibrational modes and compensation effects in Mg-doped GaN", Phys. Stat. Sol. C **0**, 1783-1794 (2003).

[16] S. M. Myers, C. H. Seager, A. F. Wright, B. L. Vaandrager, and J. S. Nelson, "Electron-beam dissociation of the MgH complex in p-type GaN", J. Appl. Phys. **92**, 6630-6635 (2002).

[17] M. A. Reshchikov, M. Vorobiov, D. O. Demchenko, Ü. Özgür, H. Morkoç, A. Lesnik, M. P. Hoffmann, F. Hörich, A. Dadgar, and A. Strittmatter, "Two charge states of the C_N acceptor in GaN: Evidence from photoluminescence", Phys. Rev. B **98**, 125207 (2018).

[18] B. McEwen, M. A. Reshchikov, E. Rocco, V. Meyers, K. Hogan, O. Andrieiev, M. Vorobiov, D. O. Demchenko, and F. Shahedipour-Sandvik, "MOCVD Growth and Characterization of Be-Doped GaN", ACS Applied Electronic Materials **4**, 3780-3785 (2022).

[19] M. A. Reshchikov, M. Vorobiov, O. Andrieiev, B. McEwen, E. Rocco, V. Meyers, D. O. Demchenko, and F. Shahedipour-Sandvik, "Photoluminescence from Be-Doped GaN Grown by Metal-Organic Chemical Vapor Deposition", Phys. Stat. Sol. (b) **260**, 2200487 (2023).

[20] M. Zajac, L. Konczewicz, M. A. Reshchikov, B. McEwen, and F. Shahedipour-Sandvik, "P-type conductivity in GaN:Be epitaxial layers", an abstract to the IWN-2024 conference, Honolulu, HI, November 3-8, 2024.

[21] M. A. Reshchikov, A. A. Kvasov, M. F. Bishop, T. McMullen, A. Usikov, V. Soukhoveev, and V. A. Dmitriev, "Tunable and abrupt thermal quenching of photoluminescence in high-resistivity Zn-doped GaN", Phys. Rev. B **84**, 075212 (2011).

[22] M. A. Reshchikov, "Measurement and analysis of photoluminescence in GaN", J. Appl. Phys. **129**, 121101 (2021).

[23] J. Heyd, G. E. Scuseria, and M. Ernzerhof, "Hybrid Functionals Based on a Screened Coulomb Potential", J. Chem. Phys. **118**, 8207–8215 (2003).

[24] D. O. Demchenko, O. Andrieiev, M. Vorobiov, M. A. Reshchikov, B. McEwen, and F. Shahedipour-Sandvik, "Physics of acceptors in GaN: Koopmans' tuned HSE hybrid functional and experiment", Phys. Rev. B **110**, 035203 (2024).

[25] M. A. Reshchikov, M. Vorobiov, O. Andrieiev, D. O. Demchenko, B. McEwen, and F. Shahedipour-Sandvik, "Dual Nature of the Be_{Ga} Acceptor in GaN: Evidence from Photoluminescence", Phys. Rev. B **108**, 075202 (2023).

[26] M. A. Reshchikov, D. O. Demchenko, B. McEwen, and F. Shahedipour-Sandvik "On the identity of the shallowest acceptor in GaN", submitted to Phys. Rev. B (manuscript BX14572).

[27] M. A. Reshchikov, "Photoluminescence from defects in GaN", Gallium Nitride Materials and Devices XVIII, ed. H. Fujioka, H. Morkoç, and U. Schwarz, Proc. SPIE **12421**, Gallium Nitride Materials and Devices XVIII, 1242109 (2023).

[28] D. O. Demchenko and M. A. Reshchikov, "Hydrogen passivation of the beryllium acceptor in GaN and a possible route for *p*-type doping", Appl. Phys. Lett. **118**, 142103 (2021).

[29] X.-R. Han, Y. Li, P. Li, X.-L. Yan, X.-Q. Wu, and B. Huang, "A comparative study of defect diffusion and recombination in Si and GaN", J. Appl. Phys. **132**, 045701 (2022).

[30] A. Kyrtsos, M. Matsubara, and E. Belotti, "Migration mechanisms and diffusion barriers of carbon and native defects in GaN", Phys. Rev. B **93**, 245201 (2016).

[31] K. Saarinen, T. Suski, I. Grzegory, and D. C. Look, "Thermal stability of isolated and complexed Ga vacancies in GaN bulk crystals", Phys. Rev. B **64**, 233201 (2001).

[32] F. Tuomisto, V. Ranki, D. C. Look, and G. C. Farlow, "Introduction and recovery of Ga and N sublattice defects in electron-irradiated GaN", Phys. Rev. B **76**, 165207 (2017).

[33] B. T. Kelly, *Irradiation Damage to Solids*, Pergamon Press, Oxford 1966, p. 179.

[34] J.-S. Park and K. J. Chang, "Diffusion and Stability of Hydrogen in Mg-doped GaN: A Density Functional Study", Appl. Phys. Express **5**, 065601 (2012).

[35] A. Castiglia, J.-F. Carlin, and N. Grandjean, "Role of stable and metastable Mg-H complexes in p-type GaN for cw blue laser diodes", Appl. Phys. Lett. **98**, 213505 (2011).

[36] T. Narita, N. Ikarashi, K. Tomita, K. Kataoka, and T. Kachi, "Wide range doping control and defect characterization of GaN layers with various Mg concentrations", J. Appl. Phys. **124**, 165706 (2018).

[37] D. Gogova, A. Kasic, H. Larsson, B. Pécz, R. Yakimova, B. Magnusson, B. Monemar, F. Tuomisto, K. Saarinen, C. Miskys, M. Stutzmann, C. Bundesmann, and M. Schubert, "Optical and structural characteristics of virtually unstrained bulk-like GaN", Jpn. J. Appl. Phys., Part 1 **43**, 1264-1268 (2004).

[38] F. Tuomisto, K. Saarinen, T. Paskova, B. Monemar, M. Bockowski, and T. Suski, "Thermal stability of in-grown vacancy defects in GaN grown by hydride vapor phase epitaxy", J. Appl. Phys. **99**, 066105 (2006).

[39] M. A. Reshchikov, D. O. Demchenko, J. D. McNamara, S. Fernández-Garrido, and R. Calarco, "Green luminescence in Mg-doped GaN", Phys. Rev. B **90**, 035207 (2014).

[40] M. A. Reshchikov, "Photoluminescence from Vacancy-Containing Defects in GaN", Phys. Stat. Sol. (a) **220**, 2200402 (2023).

[41] M. Vorobiov, O. Andrieiev, D. Demchenko, and M. A. Reshchikov, "Nitrogen vacancy-acceptor complexes in GaN" J. Appl. Phys. **135**, 155701 (2024).